

Design and performance of a system for two-dimensional readout of gas electron multiplier detectors for proton range radiography

Piotr Wiącek,
Władysław Dąbrowski,
Tomasz Fiutowski,
Bartosz Mindur,
Alicja Zielińska

Abstract. The proton range radiography (PRR) technique being developed is expected to provide significant improvements in precision delivery of the therapeutic dose in the hadron therapy. The technique requires measuring residual energies and trajectories of mono-energetic protons passing through an object to be imaged. Such an imaging system can be operated *in-situ* before and after the treatment allowing real time monitoring of the irradiated tissue position. A detector system suitable for such applications must be capable of measuring proton tracks with submillimeter spatial resolution over area of $30 \times 30 \text{ cm}^2$. In order to limit the exposure time and obtain real-time images the detector and data acquisition must provide capability of measuring high proton rates up to 10^6 s^{-1} . In this paper we present novel concept of two-dimensional (2-D) readout of the gas electron multiplier (GEM) detectors used as the position sensitive detectors. The key component of the system is an application specific integrated circuit (ASIC) named GEMROC. The GEMROC comprises 32 independent channels, each one capable of measuring the amplitude and the time of incoming signals. The positions are then reconstructed by coincidences of signals from the X- and Y-readout strips. The design and performance of the GEMROC ASIC are discussed and the results obtained for a test bench based on a smaller $10 \times 10 \text{ cm}^2$ GEM chamber are presented. The test results demonstrate clearly that with respect to the two critical parameters, i.e. the noise and the count rate capability, the developed readout system meets the requirements for clinical applications of the PRR technique.

Key words: front-end electronics • GEM detectors • 2-D imaging • proton range radiography

P. Wiącek✉, W. Dąbrowski, T. Fiutowski, B. Mindur, A. Zielińska
AGH University of Science and Technology,
Faculty of Physics and Applied Computer Science,
al. A. Mickiewicza 30, 30-059 Krakow, Poland,
Tel.: +48 12 617 2993, Fax: +48 12 634 0010,
E-mail: wiacek@agh.edu.pl

Received: 30 November 2011
Accepted: 6 March 2012

Introduction

Proton radiation therapy is one of the most precise techniques of cancer therapy. A precisely defined range of protons in the tissue allows one to deliver the maximum dose corresponding to the Bragg peak in a well defined region containing the tumor, while minimizing the parasitic dose to the surrounding healthy tissue. In order to utilize fully advantage of this technique the localization of the targeted tumor has to be known precisely. Nowadays, a standard technique used for localization of the tumor is X-ray computed tomography (CT), which has, however, several limitations. The resulting uncertainties can lead to position errors from several millimeters up to 1 cm depending on the anatomical region treated. In addition, during the treatment the patient may move and thus one needs to verify the position of the targeted tissue with respect to the beam. For both of these problems, a CT system using the protons themselves is an attractive solution. Two different detector systems specific for this method have been proposed and are under development: proton range radiography (PRR)

[2] or proton computed tomography (p-CT) [6]. Both imaging systems can utilize the same proton beam, which is used for delivering the therapeutic dose, and can be operated *in-situ* before and after the treatment allowing real time monitoring of the position of the irradiated tissue.

A detector system suitable for such applications must be capable of measuring the residual proton energy after passing through the object to be imaged and proton trajectories with submillimeter spatial resolution over the area of about of $30 \times 30 \text{ cm}^2$. In order to limit the exposure time and obtain real-time images the position sensitive detector and the data acquisition (DAQ) system must provide capability of working with a high-intensity proton beam up to 10^6 proton/s per the whole detector area. In case of using the pencil beam technique, which has been introduced recently [8], the high intensity will be localized in a small region of a few square millimeters of the detector. Several detection technologies are being investigated to realize a system meeting these requirements. The two main development lines are: a detector system employing silicon strip detectors to determine the proton trajectories and a CsI scintillating crystal to measure the residual energies of protons passing through the imaged object [6], and a system using gas electron multiplier (GEM) detectors with 2-dimensional (2-D) readout to determine trajectories of protons and a stack of 30 thin plastic scintillators, to measure the total residual energy and the range of protons passing through the object [2].

The principle of the PRR detection system, being developed in the frame of the AQUA program [9], is illustrated schematically in Fig. 1. It is worth noting that the concept of the system has been borrowed from the experimental high energy physics where a typical detector system comprises a tracking detector followed by a calorimeter. In order to reconstruct the trajectories of the protons after passing through the target at least two planes of position sensitive detectors, each one delivering two coordinates, are needed. Typical energy of the proton beam used in the hadron radiotherapy is of about 230 MeV. The position sensitive detectors should be transparent for the protons, so that the energy fraction released in these detectors is small compared with the energy of the primary beam. At the same time, the energy released in the position sensitive detectors should be sufficiently large to generate a detectable signal. Also, the position sensitive detectors should not cause scattering of the protons. Because of relatively low energy of protons used in the hadron radiation therapy compared to energies of minimum ionizing particles in the high energy physics experiments the latter constraint concerning the scattering is more severe in the proton CT compared to the high energy physics experiments.

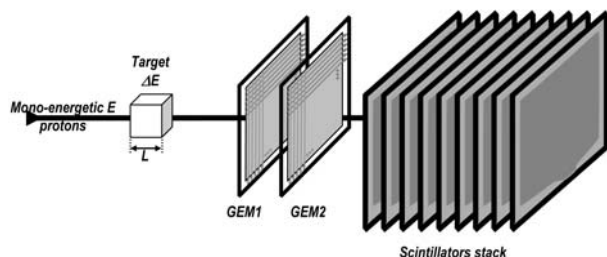


Fig. 1. Schematic diagram of the PRR detection system.

In the PRR system being developed by the TERA foundation the GEM chambers with 2-D strip readout are used as the position sensitive detectors. In this paper we present novel concept of 2-D readout system of the GEM detectors, which provides the spatial resolution and the high count rate capability as required for the PRR application.

Requirements for 2-dimensional readout of GEM chambers in the PRR system

A cross section of the GEM chamber with three stages of electron multiplication, i.e. with three GEM foils, used in the PRR system is shown schematically in Fig. 2. With the three GEM foils total electron multiplication factor of about 10^4 is achieved, which is needed to obtain measurable signals induced in the readout strips. However, each stage contributes to the spatial spreading of the electron cloud and finally the signals corresponding to one particle is induced in several readout strips. In order to estimate the position of the passing particle one needs to measure the amplitudes of signals at all collecting electrodes and find the center of gravity for each cluster of signals.

The primary charge generated by 230 MeV protons in the drift volume of the chamber has a Landau distribution with the most probable value of 0.005 fC, i.e. of 31 electrons only. After multiplication process in the three GEM foils, one obtains the most probable value of the total charge of about 50 fC, which is then divided between several strips. Combining the charge division effects and the Landau distribution of the generated charges one arrives at a conclusion that the system should be capable of detecting signals as low as 6 fC induced in individual strip. This minimum signal sets the requirement for the noise of the front-end electronics, which preferably should be kept below 1 fC rms of the equivalent input charge (ENC). Then, the discrimination threshold set at a level of 6 fC input equivalent will correspond to 6σ of noise, which will be sufficient to suppress the noise hit rate to a negligible level compared to the signal rate. This requirements appears to be not trivial for the large area chamber of $30 \times 30 \text{ cm}^2$, resulting in large input capacitances

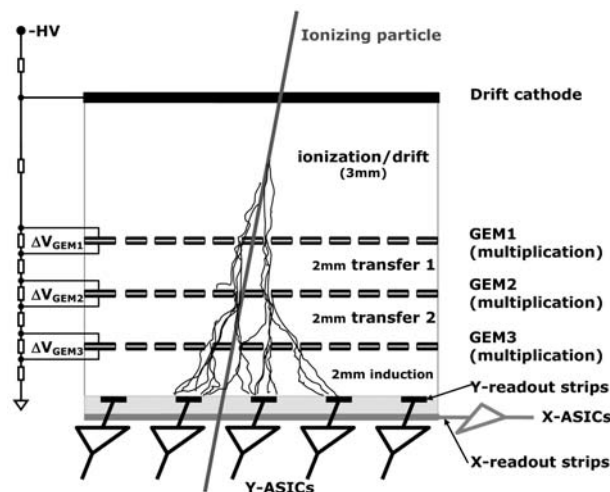


Fig. 2. Schematic cross section of the GEM chamber used in the PRR system.

Table 1. Geometrical and electrical parameters of the GEM readout strips

Parameter	Value			
	Single strip readout		Strips connected in pairs	
	Top	Bottom	Top	Bottom
Strip length	300 mm			
Strip pitch	400 μm			
Readout pitch	400 μm		800 μm	
Strip width	80 μm	340 μm	80 μm	340 μm
Capacitance of strip to other readout plane	27 pF	31 pF	54 pF	62 pF
Interstrip capacitance	2 pF	15 pF	2 pF	15 pF
Total strip capacitance of 300 mm strip	31 pF	61 pF	58 pF	92 pF
Total resistance of 300 mm strip	22 Ω	4.6 Ω	11 Ω	2.3 Ω
External input coupling capacitor	200 pF			
Input protection resistor	10–50 Ω			
Total capacitance of input protection diodes	2 pF			

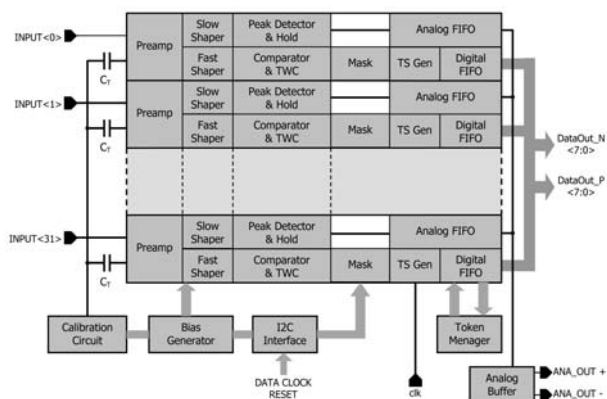
seen by the preamplifiers. The electrical parameters of the detector are summarized in Table 1 for two possible pitches of the readout electrodes, 400 or 800 μm . For the developed PRR system, a readout pitch of 800 μm has been chosen, which results in the total input capacitance of about 94 pF in the worst case. Such a high capacitance requires careful noise optimization of the front-end circuit taking into account the constraint on the power dissipation. For the chamber of $30 \times 30 \text{ cm}^2$ and readout pitch of 800 μm , one needs 384 readout channels for each coordinate so 768 readout channels in total. There are two main fundamental reasons, limited space around the chamber and the cost, for which there is no other option but to realize the front-end electronics in the form of multichannel integrated circuits.

The primary requirement of the PRR detection system, which drives the concept of the readout architecture of the GEM detectors, is the count rate capability. In order to make the developed detection system useful for clinical applications the imaging has to be performed as quickly as possible. On the other hand, in order to obtain an image of quality useful for medical interpretation one needs to collect a certain number of protons. In order to utilize fully the available intensity of the beam the GEM detector should be capable of measuring a beam of intensity of 10^6 protons per second arriving randomly and provide 2-D information about each proton position. Since the readout of X- and Y-coordinates is performed by two planes of orthogonal strips for each GEM chamber, this requires making fast coincidences between the signals recorded at X- and Y-strips. Due to spread of the charge carriers in the chamber the signals are induced in 3 to 4 strips on average for every proton passing the chamber. Thus, the pulse rate in the readout electronics is expected to be up to $4 \times 10^6 \text{ s}^{-1}$. The 2-D detectors using two sets of orthogonal strips for determining the positions are known to have severe limitations on the count rate. The systems using double-sided silicon strip detectors [7] as well as the existing readout of the GEM chambers [2] are suitable for count rates up to 10^4 s^{-1} . Thus, increasing the count rate capability by two orders of magnitude is a real challenge for our project. The maximum count rate in 2-D readout is primarily limited by the time needed to identify coincidences between the signals from X- and Y-strips belonging to the same detection

event. In order to determine the position uniquely only one particle per the whole detector area is allowed within the given coincidence window. The readout system used so far in the prototype PRR detector requires reading out the information from all X- and Y- front-end channels for each detected event and searching for coincidences in an external circuit. The larger number of channels the longer time is needed to read out the entire detector. Therefore, we have proposed novel readout architecture [3], in which the time of the signal occurrence is measured in each channel and converted to a digital number so that every detected signal receives a time stamp. Then, coincidences can be identified on-line in an advance digital processor based on an FPGA (Field Programmable Gate Array) or off-line in the DAQ system.

GEMROC – application specific integrated circuit

A key component of the readout system is an application specific integrated circuit (ASIC) named GEMROC. A schematic block diagram of the ASIC is shown in Fig. 3. Details of the circuit designs implemented in the GEMROC ASIC are given in Refs. [4, 5]. The GEMROC comprises 32 independent channels, each one capable of measuring the amplitude and the time of incoming signals. Since the signals occur randomly the primary function of each channel is to detect the incoming signals with amplitudes above the noise level independently of other channels. Such a function is

**Fig. 3.** Simplified block diagram of the GEMROC ASIC.

called self-triggering in contrast to the readout architectures used commonly in the high energy physics experiments, where usually an external trigger signal is available, which helps to track the timing sequence of signals occurring in the detector. Therefore, in the GEMROC front-end circuit the signal is split into a timing channel, which generates the trigger signal and timing information, and an energy channel, which performs the amplitude measurement. The discrimination threshold set in the timing channel defines the minimum detectable signal and so the detection efficiency, but the discrimination threshold defines also the noise hit rate. Therefore, in order to guarantee 100% detection efficiency and keep the noise hit rate at a negligible level a high signal-to-noise ratio is needed. Furthermore, the signal-to-noise ratio determines also the time jitter of the discriminator response, which is used as the timing signal. Detail analysis of the detection efficiency and of the time jitter due to electronic noise leads to a requirement for the ENC in the timing channel should be below 1 fC rms for the largest strip capacitance of 94 pF.

Figure 4 shows schematically the timing diagram of the signals in each channel. The signal amplitude in the energy channel is sensed by the peak detect and hold (PDH) circuit. The readout sequence is initiated by the response of the comparator in the timing channel. The fast timing signal is transferred to the time stamping circuit and further in the digital form as a 12-bit word to the digital FIFO (first-in-first-out) buffer, the amplitude of the signal in the energy channel is transferred to the analog FIFO buffer, and then the PDH circuit is reset to be ready for receiving next pulse.

The FIFO derandomizing buffers are read out via a token-based multiplexer, which in every cycle transfers to the output the data only from the channel, which contain data and skips the channels with no data. This way it is possible to transfer the data off the ASIC with a rate corresponding to the average data rate per 32 channels. The analog data is read out via a single differential link at a rate of 31.25 MHz. The digital data is read out via a parallel 8-bit bus at a rate of 125 MHz using the

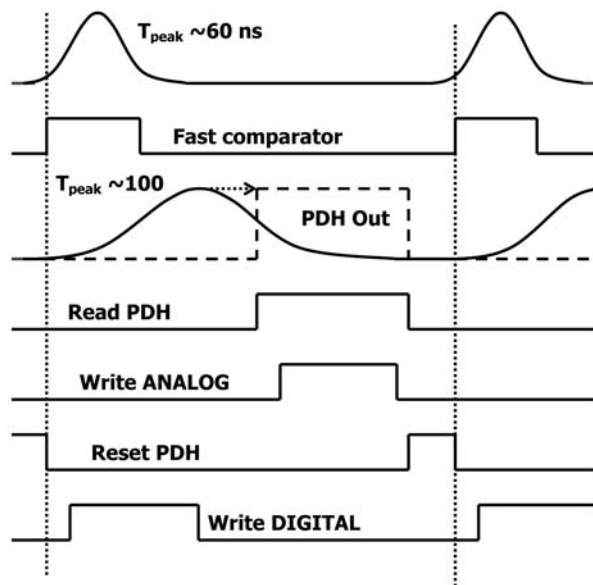


Fig. 4. Timing diagram of signals at the front-end outputs and control signals to write the data into the analog and the digital memory.

low voltage differential signaling (LVDS) standard. It should be stressed that only by employing such a readout architecture, utilizing fully data derandomization and zero suppression, one can achieve the required count rates to measure efficiently proton rates up to 10^6 s^{-1} .

The GEMROC ASIC is equipped with an internal calibration system, which allows testing and calibrating the analog circuits without employing precise external test signals. Using this functionality, all basic electrical parameters of every channel can be measured. The two critical parameters are the ENC of the timing and the energy channel, and the time resolution. The ENC as a function of the input capacitance has been measured using external discrete capacitors connected to the preamplifier inputs. The typical results for the energy and the timing channel are shown in Fig. 5a. One can see for the total input capacitance up to 120 pF the ENC for the timing channel remains below 0.5 fC, to be compared with the target design specification of 1 fC. The ENC of the energy channel is even lower for large input capacitances because of a longer peaking time of energy channel compared to the timing channel. The measurement results are consistent with the expected dependence of the ENC on the input capacitance and the peaking time [5].

The time resolution is determined by the time walk and the time jitter of the comparator. In order to mini-

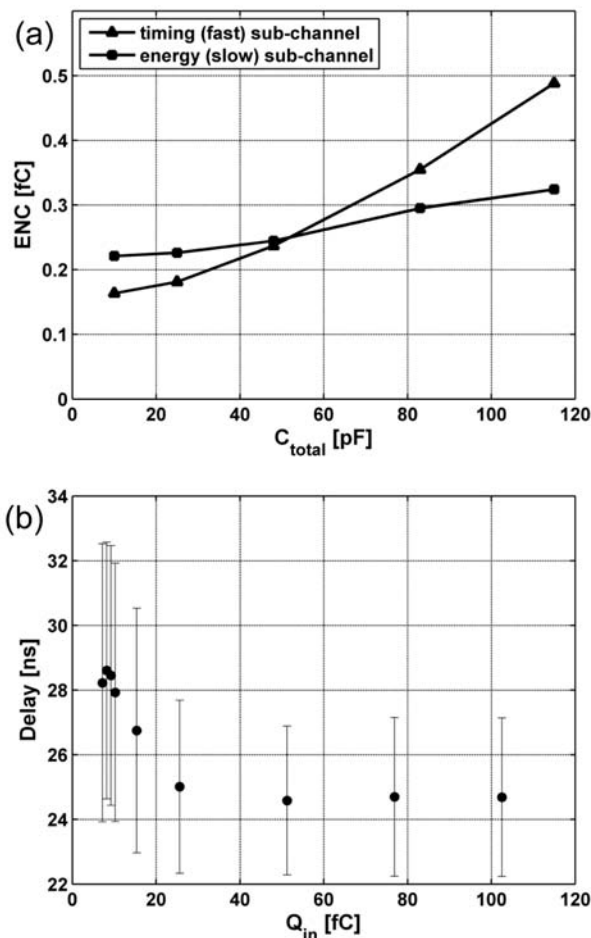


Fig. 5. Typical test results demonstrating the performance of the GEMROC ASIC: (a) ENC vs. input capacitance for the timing and the energy channel, (b) time walk and time jitter of the timing channel.

mize the time walk a time walk compensation (TWC) circuit has been implemented in the timing channel. The time resolution has been measured using two ASICs, one as a trigger providing the reference signal and other one under test. The delay vs. signal amplitude was measured as the delay between the time stamp of the trigger ASIC and the time stamp of the test ASIC. Figure 5b shows the result of such measurements for an input capacitance of 68 pF. The time walk for the input signals from 6 fC to 100 fC is of about 4 ns. The bars represent the time jitter due to noise at one sigma level. As expected, the time jitter is larger for small input signals, but it remains below 4 ns rms. For these timing parameters of the ASIC, the effective time resolution of the detector system will be determined by the time jitter of the input signals due to fluctuations of the charge collection time in the GEM chamber, which is of the order of 7 ns rms for minimum ionizing particles [1].

Test bench results

The performance of the developed readout system has been verified in the test bench using a GEM chamber of smaller area $10 \times 10 \text{ cm}^2$. Besides the area, the structure and parameters of the GEM foils as well as the bias conditions were the same as foreseen for the large area chamber. The chamber was filled with the standard gas mixture Ar/CO₂ (70/30). The readout is arranged with a pitch of 800 μm strips by connecting adjacent strips in pairs so that each side of the chamber is read out by 128 strips. A photograph of the assembled detector is shown in Fig. 6. The GEMROC ASICs are assembled on the small printed circuit boards (PCB), each one containing two ASICs. Thus, for each coordinate two such boards are needed to read out 128 strips. The data from 128 channels are multiplexed into a DAQ board containing a fast ADC (analog-to-digital converter), an FPGA, and an interface providing a fast, Ethernet protocol based, data link to a computer.

As discussed earlier, understanding the spatial distribution of the collected charge across several strips is an important aspect for position measurements and, in particular, for elaborating an optimum algorithm for estimating the most probable position using the signal amplitudes within the cluster. The developed readout system allows us to associate the signals measured at

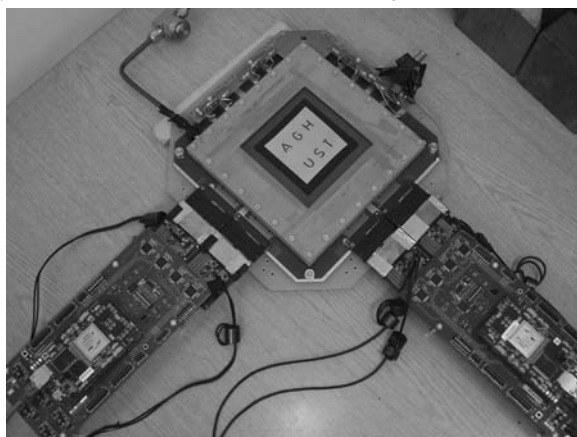


Fig. 6. $10 \times 10 \text{ cm}^2$ GEM chamber with complete readout electronics.

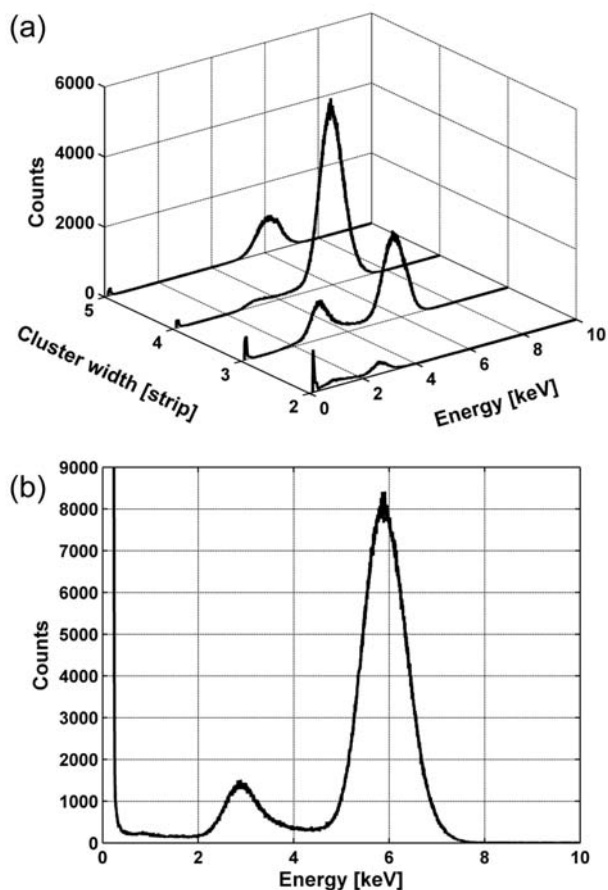


Fig. 7. Amplitude distribution measured for X-rays from a ⁵⁵Fe radioactive source. (a) Distributions including events resulting in 2-, 3-, 4-, and 5-strip wide clusters, (b) cumulative distribution including all clusters.

different strips with the given detection event according to their time stamps and so to find the distribution of signals within the clusters event by event. The results of such measurements for X-rays from a ⁵⁵Fe radioactive source are shown in Fig. 7. For each event, the strips belonging to one cluster have been identified using their time stamps and the signal amplitudes from these strips are summed to obtain the signal proportional to the total energy released in the detector volume. In Fig. 7 the energy spectra corresponding to the clusters containing 2, 3, 4, and 5 strips are plotted separately as well as the spectrum including all events. One can see that for majority of events the charge is divided between 3 or 4 strips, though the fraction of events with the charge spread across 5 strips is not negligible. Let us note that the 5-strip clusters have practically no escape peak corresponding to ArK_α fluorescence X-rays. Such events may occur if the excited Ar atoms emit Auger electrons parallel to the detector plane and result in wider distributions of the generated charge cloud. The amplitude distribution of 2-strip clusters includes events with much lower energy deposition. Using the timing information provided by the GEMROC ASICs, one can reject such events when building the energy spectrum of the measured radiation, however, for the spatial analysis they are useful as long as the signal on individual strip are well separated from the noise.

Since the signals recorded on X- and Y-strips corresponding to the given detection event are clustered

according to their time stamps the time resolution, including fluctuation of the charge collection time in the GEM chamber, is a parameter that will determine the maximum rate of protons. Within a given time window only one photon or particle is allowed in the whole detector in order to avoid ambiguity in reconstruction of the position. Figure 8 shows the distribution of the time stamp differences between the maximum signals within the clusters recorded in X- and Y-strips. A Gaussian fit to the measured distribution gives the time resolution of about 12 ns rms, which confirms that both, the time jitter of the input signal and the time jitter of the discriminator response due to electronic noise, contribute to the time resolution of the effective time resolution of the system. The distribution is not fully symmetric and is shifted with respect to zero. The shift is partially caused by the delay of about 4 ns in the external cable providing synchronization between the signals from the X- and Y-strips. Further shift and asymmetry of the distribution shown in Fig. 8 is most likely due to different geometry of the X- and Y-readout strips resulting in different distribution of the electric field and so in a systematic difference of the shapes of the induced current signals. To ensure equal charge sharing between the upper and the lower coordinates the width of the strips is 80 μm in the top plane and 340 μm in the bottom plane [1]. In such a geometry the readout strips in the bottom readout plane (X-strips in Fig. 2) are partially shielded by the strips in the top readout plane (Y-strips in Fig. 2) so the signals induced in the bottom strips are systematically delayed with respect to the signals induced in the top strips. This systematic shift is small compared to other statistical fluctuations and does not affect the count rate capability of the detector.

The ultimate application of the developed system is 2-D imaging. In order to demonstrate the proof of principle for the prototype detector readout system we have performed a simple imaging test using X-rays from a ^{55}Fe radioactive source. The window of the chamber was covered with a brass plate of area $8 \times 8 \text{ cm}^2$ with the letters "AGH UST" cut out. The plate is visible in the photo shown in Fig. 6. The width of the cut out was of about 2 mm. During that measurement, the rate of recon-

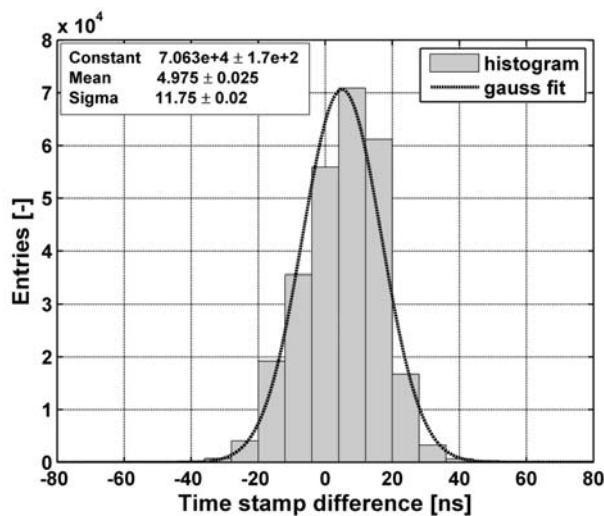


Fig. 8. Distribution of time stamp differences between hits recorded in X- and Y-plane for X-rays from a ^{55}Fe radioactive source.

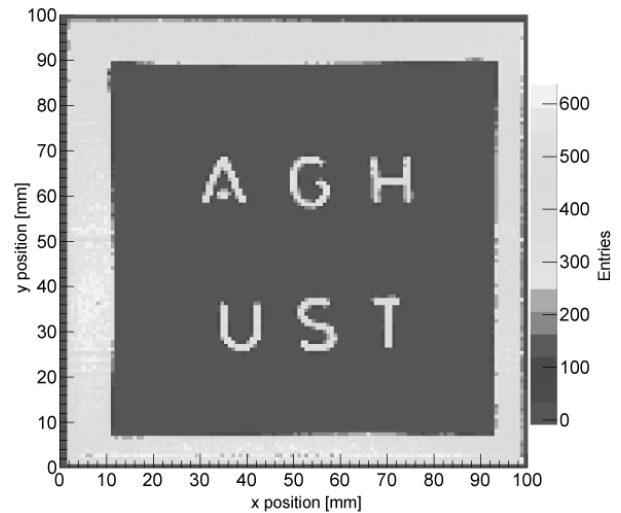


Fig. 9. Example 2-D image obtained with a standard GEM chamber and the developed readout system using X-rays.

structed events was of about $2.6 \times 10^4 \text{ s}^{-1}$ since most of the detector area was shielded by the plate. Given the pitch of readout strips of 0.8 mm the basic pixel size of the image is $0.8 \times 0.8 \text{ mm}^2$. The obtained image is shown in Fig. 9. This picture, although qualitative, demonstrates the performance of the readout system. The plot shows the spatial distribution of the reconstructed event counts without any corrections. It should be noted that the background is very uniform and there are no noisy spots reconstructed in the shielded area. Also, the boundaries between the detector regions readout by particular ASICs are not noticeable. When evaluating the quality of the image one should keep in mind that the X-ray source was placed at a distance of about $\sim 30 \text{ cm}$ above the detector and there was no collimator used in order to obtain uniform illumination of the whole detector area. However, in such a geometry the image quality is affected by scattering of X-rays and by the parallax. Therefore, the edges of the cut outs are not particularly sharp in the obtained image and should not be interpreted in term of the spatial resolution of the detector.

Summary

In the paper we have presented the concept and a prototype system for readout of 2-D GEM detectors. The system has been designed to meet the requirement for the position sensitive detectors based on GEM chambers to be used in clinical applications of the PRR technique. The core of the readout system is the multichannel GEMROC ASIC allowing for simultaneous measurements of amplitude and time for each recorded pulse. The readout architecture employing on-chip zero suppression and data derandomization makes the developed ASIC suitable for readout of 2-D strip detectors at high count rates. The test results confirm that the developed GEMROC ASICs and the DAQ system are fully functional and fulfill the requirements for the readout of the 2-D GEM detector. The novel readout architecture implemented in the GEMROC ASICs can be accommodated to other types of detectors, e.g. double-sided silicon strip detectors, after proper optimization of the front-end for a given detector parameters.

Acknowledgment. This work was supported partially by the Polish Ministry of Science and Higher Education and its grants for Scientific Research. We thank F. Sauli from the TERA Foundation for valuable discussion on the design specifications and for providing financial support for ASIC manufacturing.

References

1. Altunbas A, Capéans M, Dehmelt K *et al.* (2002) Construction, test and commissioning of the triple-gem tracking detector for compass. *Nucl Instrum Methods A* 490:177–203
2. Amaldi U, Bianchi A, Chang Y-H *et al.* (2011) Construction, test and operation of a proton range radiography system. *Nucl Instrum Methods A* 629;1:337–344
3. Brogna AS, Buzzetti S, Dąbrowski W *et al.* (2008) MSGCROC – an ASIC for high count rate readout of position sensitive microstrip gas chambers for thermal neutrons. In: 2008 IEEE Nuclear Science Symp Conf Record, N11-2:1482–1488
4. Dąbrowski W, Fiutowski T, Mindur B, Wiącek P, Zielińska A (2011) Development of an ASIC for 2-D readout of gas electron multiplier detectors. In: Proc of the 18th Int Conf Mixed Design of Integrated Circuits and Systems, MIXDES 2011:303–308
5. Fiutowski T, Dąbrowski W, Mindur B, Wiącek P, Zielińska A (2011) Design and performance of the GEMROC ASIC for 2-D readout of gas electron multiplier detectors. In: 2011 IEEE Nuclear Science Symp Conf Record: 1540–1544
6. Menichelli D, Bruzzi M, Bucciolini M *et al.* (2010) Characterization of a silicon strip detector and a YAG:Ce calorimeter for a proton computed radiography apparatus. *IEEE Trans Nucl Sci* 57:8–16
7. Overdick M, Czermak A, Fischer P *et al.* (1997) A “Bioscope” system using double-sided silicon strip detectors and self-triggering read-out chips. *Nucl Instrum Methods A* 392;1/3:173–177
8. Pedroni E, Scheib S, Böhringer T *et al.* (2005) Experimental characterization and physical model link of the dose distribution of scanned proton pencil beams. *Phys Med Biol* 50:541–561
9. Sistema AQUA: Advanced Quality Assurance for CNAO. <http://project-aqua.web.cern.ch/project-aqua>